1st Croatian Conference on Earthquake Engineering
1CroCEE
22-24 March 2021 Zagreb, Croatia

DOI: https://doi.org/10.5592/CO/1CroCEE.2021.122

Cyclic and monotonic moment-rotation behaviour of CFS web-connected beam-to-column joints

Ioannis Papargyriou[1], Seyed Mohammad Mojtabaei[2], Iman Hajirasouliha[3], Jurgen Becque[4]

[1] *PhD student*, Department of Civil and Structural Engineering, The University of Sheffield, UK, *i.papargyriou@sheffield.ac.uk*
[2] Department of Civil and Structural Engineering, The University of Sheffield, UK, *smmojtabaei1@sheffield.ac.uk*
[3] *Senior Lecturer*, Department of Civil and Structural Engineering, The University of Sheffield, UK, *i.hajirasouliha@sheffield.ac.uk*
[4] *Lecturer*, Department of Engineering, University of Cambridge, UK, *jurgen.becque@eng.cam.ac.uk*

Abstract

Over the past decade, the market for cold-formed steel (CFS) systems has significantly expanded, especially for the construction of low to mid-rise buildings. CFS moment-resisting frame systems have become popular even in seismic-prone regions, mainly for single-storey portal-framed buildings of industrial use. However, their application in multi-storey structures is still limited by the behaviour of the beam-to-column joints, which are prone to premature local buckling failure of the connected elements. This study aimed to develop a more practical type of moment-resisting CFS joint, which is fast and easy to assemble, while providing satisfactory seismic performance. In the proposed connection system, the beam and column elements are built-up from CFS channels and their webs are bolted to a web through-plate. In a first step, the seismic moment-rotation behaviour of CFS beam-column joints with various configurations was investigated. Detailed FE models were developed in ABAQUS, taking into account material nonlinearity and geometric imperfections, which were validated against available experimental data. The validated FE models were subsequently used to perform monotonic and cyclic analyses of CFS bolted joints with different beam slenderness values, and various web through-plate shapes and slenderness values. The moment-rotation behaviour of the studied joints was then evaluated in terms of its seismic characteristics, including bending moment capacity, rotational stiffness, ductility, energy dissipation capacity and damping coefficient. Finally, following comparison of the results, more structurally efficient CFS bolted joints suitable for multi-storey moment-resisting frame systems in earthquake regions were proposed.

Key words: Cold-formed steel (CFS), Bolted moment-resisting connections, FE analysis, Stiffness, Ductility

1 Introduction

Cold-formed steel (CFS) systems have become a popular option in the construction industry, offering tangible benefits, such as low material use, speedy erection, high strength-to-weight ratios and durability. CFS moment-resistant frame systems are currently seeing an uptake even in seismic-prone regions, mainly for single-storey, industrial-use portal frame buildings. However, their application in multi-storey structures is still mainly limited by the behaviour of the beam-to-column joints, which are prone to premature buckling failure of the connecting plate elements. These joints generally include a bolted gusset plate, which connects the beam and column webs.

Although limited research has been conducted so far on this type of connections, preliminary indications point to potentially satisfactory use in seismic applications. Experiments under monotonic loading, conducted by Chung and Lau [1] and Wong and Chung [2], have demonstrated that through-plate connections can be used in CFS moment-resisting frames, reaching a bending moment resistance equal to 42-84 % of the beam capacity. However, experiments on portal frame joints, conducted by Lim and Nethercot [3] and Dubina et al. [4] showed premature local buckling of the beam web, which led to a rapid drop in the frame capacity. In experimental and analytical work conducted by Mojtabaei et al. [5], a CFS portal frame was shown to be able to achieve 4 % inter-storey drift, thus classifying as a Special Moment Frame (SMF), as per AISC 314-16 [6]. Sabbagh [7] and Sabbagh et al. [8,9] also studied the structural performance of CFS beam-column joint assemblies under cyclic loading. The results of their studies showed that using curved flanges and additional vertical stiffeners can improve the bending moment capacity and ductility of the joints by 35 % and 75 %, respectively. According to the rotational rigidity, they classified their tested connections as either semi-rigid or rigid according to EC3 [10].

The present study aimed to develop a new type of CFS moment-resisting joint that provides improved seismic performance, while being fast and easy to assemble and install. The proposed connection system comprises back-to-back channel beam and column elements, connected through a bolted gusset plate passing between their webs. Various joint configurations were numerically investigated and, based on their moment-rotation behaviour, the best design solution was determined. For this purpose, detailed FE models were developed in ABAQUS, allowing for material nonlinearities and geometric imperfections. After validation against experimental results, parametric studies of the behaviour of joints with different web through-plate geometries and thicknesses and various beam web slenderness ratios were conducted. Their seismic characteristics were evaluated under monotonic and cyclic loading in terms of bending moment capacity, rotational stiffness, ductility, energy dissipation capacity and damping coefficient. Drawing on the conclusions, more efficient CFS bolted joints were proposed for use in multi-storey moment-resisting frames in earthquake regions.

2 Numerical model and validation

A detailed FE model was developed in ABAQUS [11] and validated against experiments A1 and B1, reported by Sabbagh in [7]. The test set-up comprised a cantilever beam, connected to a column stub, as shown in Figure 1. The general purpose S4R element was used, which has previously been proven to accurately capture the flexural response of CFS assemblies [5,12–16]. Following a mesh sensitivity analysis, a mesh size of 10 × 10 mm was adopted, balancing high numerical accuracy against manageable computational demands.

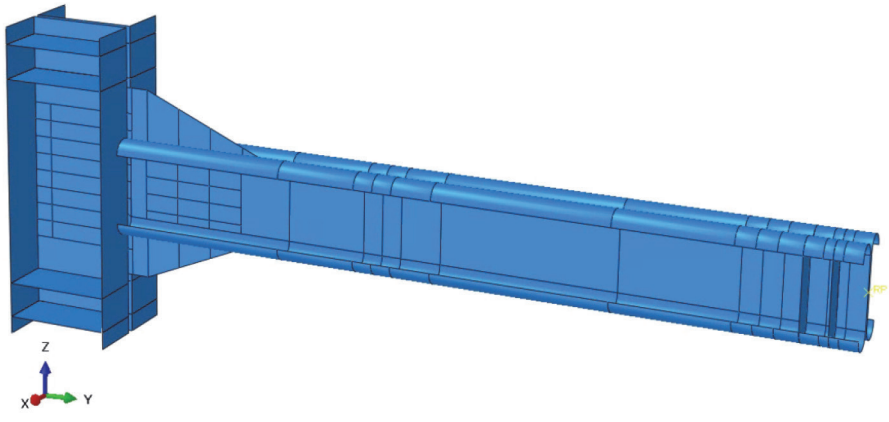

Figure 1. FE model

The beam and column consisted of two CFS channel sections, whose webs were connected back-to-back through a bolted gusset plate. The beam flanges were curved, as shown in Fig. 1. A cross-section with substantial thickness (10 mm) was chosen for the column, so it would remain elastic throughout the whole loading range. Stiffeners were rigidly connected to the column and the beam ends, to prevent local buckling at those locations. The beam was also laterally restrained at several locations against out-of-plane deformation. The loading was applied as a vertical displacement at a reference point, placed at the centroid of the beam end section. In the cyclic analyses, the loading protocol prescribed by AISC 341-16 [17], shown in Figure 2, was adopted. The nonlinear material properties were used in the model, with f_y = 313 MPa and f_u = 479 MPa for the beam and f_y = 308 MPa and f_u = 474 MPa for the gusset plate; initial geometric imperfections were generated through an elastic eigenvalue buckling analysis. The bolt behaviour was modelled with discrete fasteners, which use attachment lines between the connected surfaces. Around the fastening points, an influence radius of 8 mm was defined, equal to half the bolt diameter. The connectors between the gusset plate and the column were set to behave rigidly, whereas for the connectors connecting the gusset plate and the beam, friction and bearing behaviour were defined.

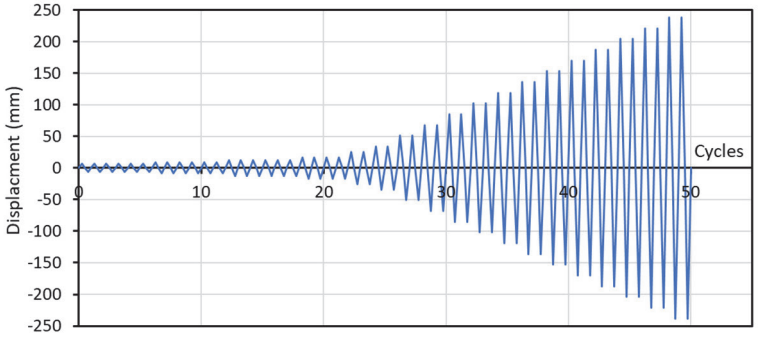

Figure 2. Cyclic loading protocol, adopted from AISC 341-16

The Static General Analysis option provided by ABAQUS was employed and the analyses were carried out using the High-Performance Computing (HPC) facilities at the University of Sheffield. Fig. 3 compares the FE model output to the experimental data for the CFS bolted connection tested by Sabbagh et al. [7]. It shows the ratio of the applied bending moment over the plastic moment of the CFS beam (M/M_p) versus the rotations, as obtained from the experiment and the detailed FE model under both cyclic and monotonic loading conditions. The rotation of the connection was determined as the ratio of beam tip displacement to the length of the beam up to the edge of the gusset plate. In general, it is seen that the FE model was able to simulate the behaviour of the connection with good accuracy over the whole loading range.

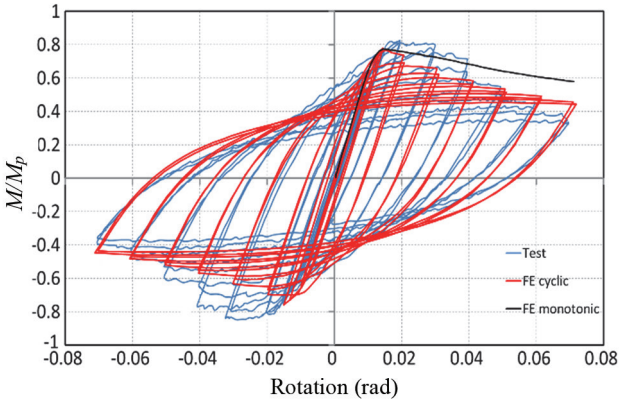

Figure 3. Comparison between test results and FE analyses of a CFS connection

3 Performance under monotonic loading

The previously validated numerical model was used to study different CFS beam-column joint configurations, shown in Figure 4, deemed suitable for multi-storey moment-resisting CFS frames. Based on the shape of the through-plate, three groups of models were considered, namely: Group A, where the through-plate was T-shaped; Group B, where the through-plate had rounded corners, and Group C, where the through-plate was approximately triangular (Figure 4). The column thickness remained at 10 mm in all analyses, while the beam thickness (t_b) was varied between 1, 2, 4 and 6 mm. The gusset plate thickness (t_g) was a multiple of the beam thickness, and equal to ($1.5 \times t_b$) or ($2.0 \times t_b$).

The efficiency of the design solutions was evaluated based on the bending moment capacity, ultimate rotation and rotational stiffness, derived from the moment-rotation responses. The (M_{max}/M_{Rb}) ratio was calculated, where (M_{max}) stands for the maximum bending moment capacity of the connection and (M_{Rb}) represents the bending moment capacity of the beam cross-section, both calculated using FE models. The beam cross-section classes were calculated to be Class 4 for (t_b = 1 mm), Class 3 for (t_b = 2 mm), Class 2 for (t_b = 4 mm), and Class 1 for (t_b = 6 mm), in accordance with Eurocode 3 [18].

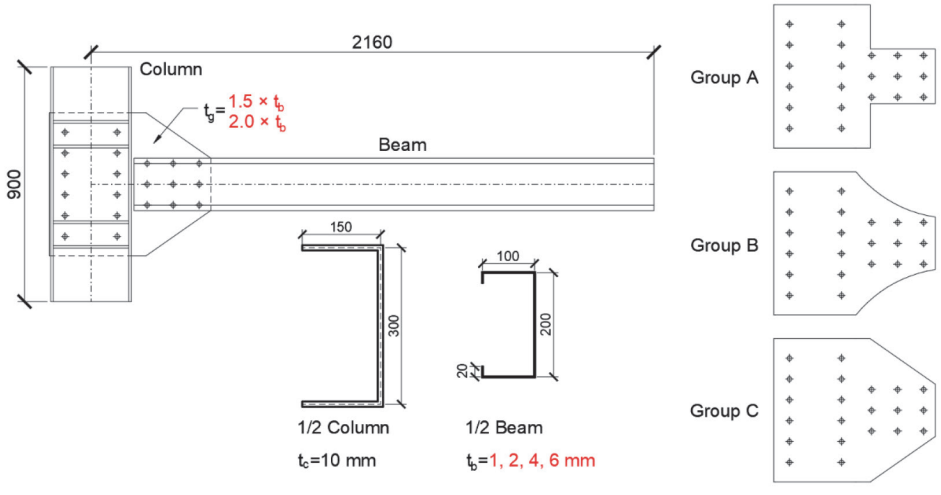

Figure 4. Beam-column joint geometry

The joints were also classified based on the criteria of AISC 341-16 [17] for seismic applications. This standard imposes various design and detailing requirements for structural members and connections in moment-resisting frames, related to their inelastic deformation capacity. It distinguishes between three categories: Special Moment Frames (SMF), with a minimum storey drift angle (θ = 0.04 rad), Intermediate Moment Frames (IMF), with storey drift angles ($0.02 \leq \theta < 0.04$ rad), and Ordinary Moment Frames (OMF), with ($\theta < 0.02$ rad).

In addition, a classification of the joints based on the provisions of EN 1993-1-8 [10] was carried out, where three classes are considered according to defined limits of the initial stiffness ($S_{j,ini}$): Rigid (R), Semi-rigid (S-R) and Pinned (P). The initial stiffness was calculated as the secant slope of the moment-rotation curve at a value of 2/3 × $M_{j,R}$, where ($M_{j,R}$) is the bending moment capacity of the joint. A joint classifies as Rigid if the initial stiffness ($S_{j,ini} \geq k_b \times E \times I_b / L_b$), where k_b = 25 for cases where there is no bracing system. (E) stands for the elastic modulus, (I_b) is the second moment of area of the beam and (L_b) represents the span length between the column centre lines. If the initial stiffness ($S_{j,ini} \leq 0.5 \times E \times I_b / L_b$), the joint classifies as Pinned. For the intermediate values the joint is considered to be Semi-rigid.

Figure 5 depicts the moment-rotation curves of the Group A, B and C joints, for beam thicknesses (t_b) of 1, 2, 4 and 6 mm and gusset plate thicknesses (t_g = 1.5 × t_b) and (t_g = 2 × t_b). Table 1 summarises the (M_{max}/M_{Rb}) ratios, along with the AISC 341-16 and EN 1993-1-8 classes. Group A joints developed the lowest bending moment resistance, with the (M_{max}/M_{Rb}) ratio not exceeding 0.33. On the other hand, Group B and C joints reached similar bending moment capacities for a gusset plate thickness (t_g = 2 × t_b). For (t_b = 1 mm) the (M_{max}/M_{Rb}) ratio was 0.67, whereas for (t_b = 2 mm to t_b = 6 mm) this ratio achieved values between 0.80 to 0.90.

All joints with beam thicknesses (t_b = 4 mm and t_b = 6 mm) exceeded rotations of 0.04 rad, classifying as SMFs. Joints in Group C with beam thicknesses (t_b = 1 mm and t_b = 2 mm) reached ultimate rotations greater than 0.02 rad, qualifying as IMFs, whereas Group A and B joints, for the same beam thicknesses, qualified predominantly as OMFs. Group A and B joints also classified as Semi-rigid for all beam and gusset plate thicknesses, whereas Group C joints exhibited Rigid behaviour for beam thicknesses (t_b = 1 mm and t_b = 2 mm), and Semi-rigid behaviour for beam thicknesses (t_b = 4 mm and t_b = 6 mm).

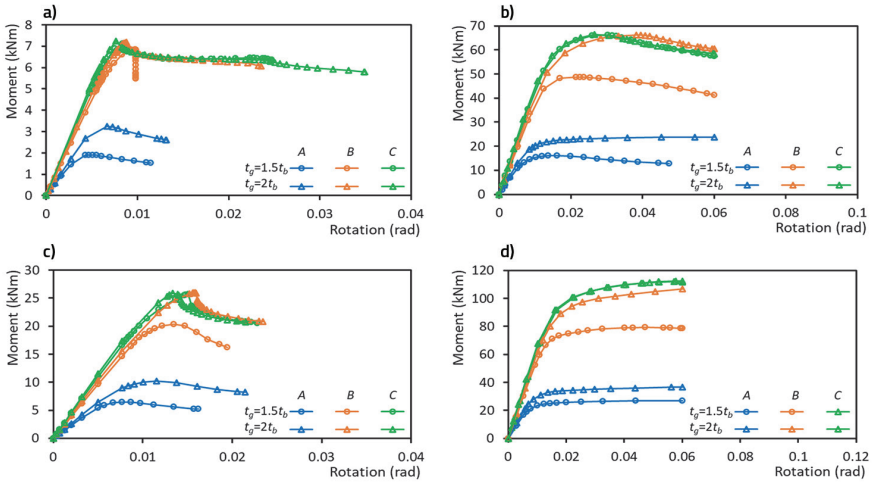

Figure 5. Moment-rotation curves of joints with beam thicknesses t_b: a) 1 mm, b) 2 mm, c) 4 mm, d) 6 mm

Table 1. Moment capacity ratios and joint classification per AISC 341-16 and EN 1993-1-8

Beam thickness t_b	Plate thickness t_g	Group A			Group B			Group C		
		$\frac{M_{max}}{M_{Rb}}$	AISC Class	EC3 Class	$\frac{M_{max}}{M_{Rb}}$	AISC Class	EC3 Class	$\frac{M_{max}}{M_{Rb}}$	AISC Class	EC3 Class
1 mm	$1.5\times t_b$	0.18	OMF	S-R	0.63	OMF	S-R	0.66	IMF	R
	$2\times t_b$	0.30	OMF	S-R	0.67	IMF	S-R	0.67	IMF	R
2 mm	1.5×tb	0.20	OMF	S-R	0.62	OMF	S-R	0.78	IMF	R
	2×tb	0.31	IMF	S-R	0.79	IMF	S-R	0.79	IMF	R
4 mm	$1.5\times t_b$	0.20	SMF	S-R	0.60	SMF	S-R	0.82	SMF	S-R
	$2\times t_b$	0.29	SMF	S-R	0.82	SMF	S-R	0.82	SMF	R
6 mm	$1.5\times t_b$	0.22	SMF	S-R	0.64	SMF	S-R	0.90	SMF	S-R
	$2\times t_b$	0.33	SMF	S-R	0.89	SMF	S-R	0.91	SMF	S-R

4 Performance under cyclic loading

Among the three joint groups A, B and C, the Group B connections with a gusset plate thickness of ($t_g = 2 \times t_b$) were selected to further have their performance evaluated under cyclic loading. Based on the monotonic responses, they performed well in terms of bending moment capacity, ultimate rotation, and rotational stiffness, while their concave shape offers more flexibility when installing the floor system.

The various design options were evaluated with respect to their moment-rotation response, rotational ductility, energy dissipation and equivalent damping coefficient. The ductility was calculated as ($\mu_\phi = \phi_u/\phi_y$), where (ϕ_u) is the ultimate rotation and (ϕ_y) is the rotation at yield. The ultimate rotation (ϕ_u) was taken as the minimum of the rotation corresponding to a 20 % drop from the maximum moment (M_{max}) or 0.06 rad, as specified by FEMA 350 [19]. The rotation at yield (ϕ_y) was determined from a bilinear approximation of the backbone curve, based on the recommendations of FEMA 356 [20]. The dissipated energy is the total area contributed by all cycles in the moment-rotation curve, up to the ultimate point. Finally, the equivalent damping coefficient expresses the loss of energy per cycle, and for any cycle, it is calculated by equating the dissipated energy in the hysteresis loop with the energy dissipated in viscous damping [21]. In this study, the cycles of primary interest corresponded to the maximum moment and the ultimate point, respectively.

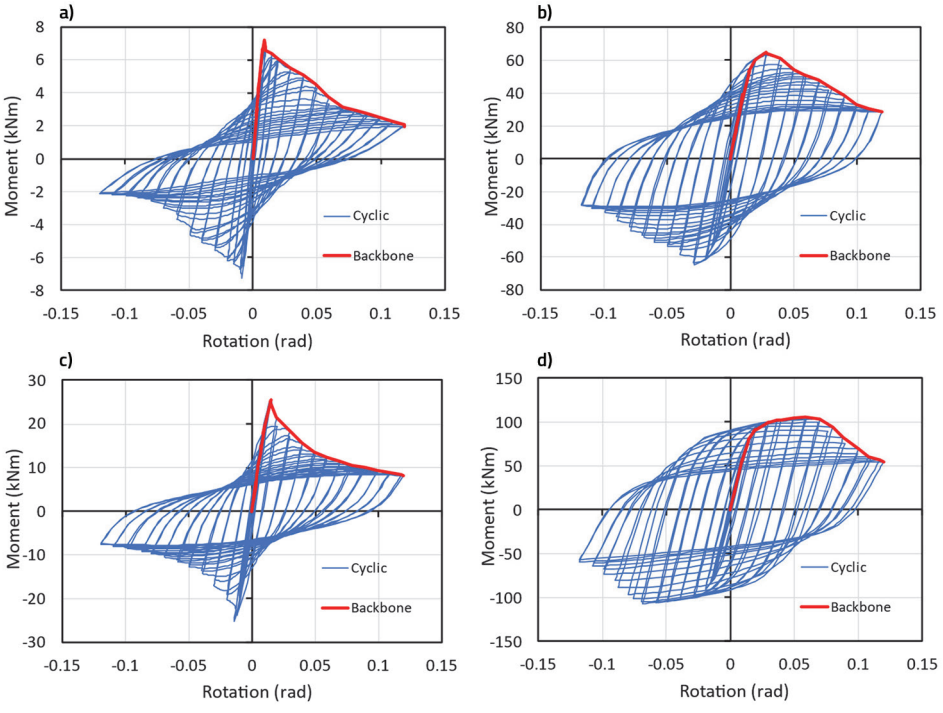

Figure 6. Moment-rotation curves of Group B joints with beam thicknesses t_b of a) 1 mm, b) 2 mm, c) 4 mm and d) 6 mm and a gusset plate thickness of $2 \times t_b$

Figure 6 presents the cyclic moment-rotation curves of the Group B joints with beam thicknesses (t_b) of 1, 2, 4 and 6 mm and gusset plate thicknesses ($t_g = 2 \times t_b$), alongside the corresponding backbone curves. The joints with thicknesses (t_b = 1, 2 and 4 mm) experienced significant plastic strength degradation after reaching their maximum moment capacity, while the joint with t_b = 6 mm was the only connection undergoing plastic strain hardening. As an example, Figure 7 depicts the local buckling failure mode of the joint with beam thickness (t_b = 4 mm).

Table 2 shows the values of the ductility, the dissipated energy and the equivalent damping coefficient for the studied connections. The ductility is greater than 4, except for a beam thickness equal to 2 mm. The dissipated energy was very low for the beams with thicknesses (t_b = 1 mm and t_b = 2 mm), but increased dramatically for (t_b = 4 mm and t_b = 6 mm). It was also observed that the equivalent damping coefficients corresponding to the ultimate cycle were almost 60 % greater than the values corresponding to the maximum moment cycle for joints with beam thicknesses (t_b = 2 mm and t_b = 4 mm). For the beam with 1 mm thickness, on the other hand, the damping coefficient was roughly five times lower at the maximum moment cycle than in the ultimate cycle, whereas for the beam with 6 mm thickness both values were very similar. From the above, it can be concluded that the most suitable joints for seismic applications were those with beam thicknesses ≥ 4 mm.

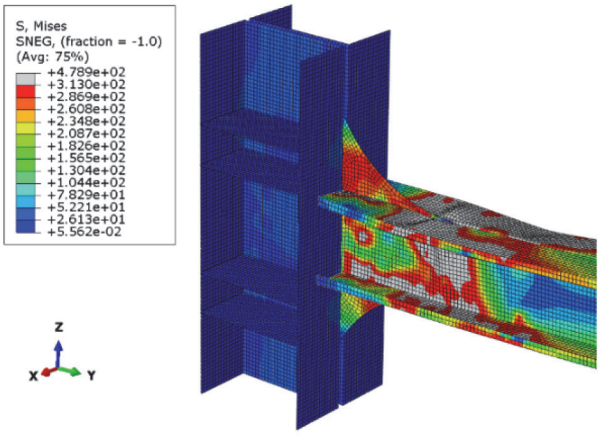

Figure 7. Failure mode and von Mises stresses in a joint with beam thickness (t_b = 4 mm)

Table 2. Ductility, dissipated energy and equivalent damping coefficients

Beam thickness t_b	Plate thickness t_g	$\mu = \frac{\phi_u}{\phi_y}$	Dissipated Energy [kJ]	Damping coefficient[kJ]	
				M_{max}	$0.8M_{max}$ or ϕ_u = 0.06 rad
1 mm	$2\times t_b$	4.5	1.01	8.4 %	40.2 %
2 mm		2	2.51	27.4 %	43.4 %
4 mm		4.3	28.86	21.9 %	35.1 %
6 mm		4.2	78.57	38.6 %	38.6 %

5 Conclusions

This work aimed to develop a new type of moment-resisting CFS joint, which is easy and fast to assemble, while providing good seismic performance. A detailed numerical model of a CFS beam-column joint was developed in ABAQUS, accounting for material nonlinearities and initial geometric imperfections. The beam and column elements consisted of double channels, connected back-to-back through their webs, while the beam-column connection was made by a bolted gusset plate. The developed model was validated against experimental results, and further used to study the effects of various geometric configurations and beam and gusset plate thicknesses on the seismic performance of the connection. A Group A of connections had T-shaped gusset plates, Group B had gusset plates with rounded corners, and Group C had approximately triangular gusset plates. The most suitable connection configuration for multi-storey moment-resisting frames in seismic regions was deemed to be the Group B design solution with a beam thickness greater than 4 mm (Class 1 and 2) and a gusset plate with rounded corners. This connection combines high moment capacity, ductility, energy dissipation and equivalent damping coefficient and facilitates construction.

References

[1] Chung, K., Lau, L., (1999): Experimental investigation on bolted moment connections among cold formed steel members, Eng. Struct. 21 898–911. doi:https://doi.org/10.1016/S0141-0296(98)00043-1.

[2] Wong, M.F. Chung, K.F. (2002): Structural behaviour of bolted moment connections in cold-formed steel beam-column, 58 253–274. doi:https://doi.org/10.1016/S0143-974X(01)00044-X.

[3] Lim, J.B.P. Nethercot, D.A. (2003): Ultimate strength of bolted moment-connections between cold-formed steel members, Thin-Walled Struct. 41 1019–1039. doi:https://doi.org/10.1016/S0263-8231(03)00045-4.

[4] Dubina, D. Stratan, A. Nagy, Z. (2009): Full - Scale tests on cold-formed steel pitched-roof portal frames with bolted joints, Adv. Steel Constr. 5 175–194.

[5] Mojtabaei, S.M. Kabir, M.Z. Hajirasouliha, I. Kargar, M. (2018): Analytical and experimental study on the seismic performance of cold-formed steel frames, J. Constr. Steel Res. 143 18–31. doi:https://doi.org/10.1016/j.jcsr.2017.12.013.

[6] American Institute of Steel Construction, Seismic Provisions for Structural Steel Buildings, Seism. Provisions Struct. Steel Build. (2010) 402. doi:111.

[7] Sabbagh, A.B. (2011): Cold Formed Steel Elements for Earthquake Resistant Moment Frame Buildings, PhD Thesis, The University of Sheffield,

[8] Bagheri Sabbagh, A., Petkovski, M., Pilakoutas, K., Mirghaderi, R. (2012): Experimental work on cold-formed steel elements for earthquake resilient moment frame buildings, Eng. Struct. 42 371–386. doi:https://doi.org/10.1016/j.engstruct.2012.04.025.

[9] Bagheri Sabbagh, A., Petkovski, M., Pilakoutas, K., Mirghaderi, R. (2013): Cyclic behaviour of bolted cold-formed steel moment connections: FE modelling including slip, J. Constr. Steel Res. 80 100–108. doi:https://doi.org/10.1016/j.jcsr.2012.09.010.

[10] CEN, Eurocode 3: Design of steel structures - Part 1-8: Design of joints, European Committee for Standardization, (2005).

[11] Dassault Systèmes Simulia, Abaqus 6.14 CAE User Guide, (2014).

[12] Mojtabaei, S.M., Becque, J., Hajirasouliha, I. (2020): Local Buckling in Cold-Formed Steel Moment-Resisting Bolted Connections: Behavior, Capacity, and Design, J. Struct. Eng. 146 04020167. doi:https://doi.org/10.1061/(ASCE)ST.1943-541X.0002730.

[13] Ye, J., Mojtabaei,S.M., Hajirasouliha, I., Pilakoutas, K. (2019): Efficient design of cold-formed steel bolted-moment connections for earthquake resistant frames, Thin-Walled Struct. 0–1. doi:https://doi.org/10.1016/j.tws.2018.12.015.

[14] Mojtabaei, S.M., Becque, J., Hajirasouliha, I. (2021): Behaviour and design of cold-formed steel bolted connections under combined actions, J. Struct. Eng. (2021) 04021013–1. doi:https://doi.org/10.1061/(ASCE)ST.1943-541X.0002966.

[15] Phan, D.T., Mojtabaei, S.M., Hajirasouliha, I., Lau, T.L., Lim, J.B.P. (2020): Design and Optimization of Cold-Formed Steel Sections in Bolted Moment Connections Considering Bimoment, J. Struct. Eng. 146 (2020) 04020153. doi:https://doi.org/10.1061/(ASCE)ST.1943-541X.0002715.

[16] Ye, J., Mojtabaei, S.M., Hajirasouliha, I. (2019): Seismic performance of cold-formed steel bolted moment connections with bolting friction-slip mechanism, J. Constr. Steel Res. 156 (2019) 122–136. doi:https://doi.org/10.1016/j.jcsr.2019.01.013.

[17] American Institute of Steel Construction (AISC), Seismic Provisions for Structural Steel Buildings, ANSI/AISC 341-16, (2016).

[18] CEN, Eurocode 3: Design of steel structures - Part 1-1: General rules and rules for buildings, European Committee for Standardization, (2010).

[19] FEMA 350, Recommended Seismic Design Criteria for New Steel Moment-Frame Buildings, (2000).

[20] FEMA 356, Prestandard and Commentary for the Seismic Rehabilitation of Building, Washington, D.C., (2000).

[21] Chopra, A. (2001): Dynamics of structures: Theory and applications to earthquake engineering, 2nd edition, Prentice Hall, (2001).